

Experimental Performance of an Adaptive Digital Linearized Power Amplifier.

Andrew S. Wright and Willem G. Durtler

Advanced Technology Development.
NovAtel Communications Ltd.
1020 - 64th Ave NE.
Calgary, Alberta, Canada.

Abstract.

High power amplification of linear modulation schemes which exhibit fluctuating envelopes, invariably leads to the generation of distortion and intermodulation products. Recent theoretical work has suggested that a complex gain predistorter may be employed to linearize a non-linear power amplifier. This paper presents experimental results demonstrating that a reduction in out-of-band spectral emissions in excess of 20 dB may be achieved by employing digital feedback and a complex gain predistorter.

I. Introduction.

The proposed North American digital cellular telephony service employs a $\pi/4$ Differential Quadrature Phase Shift Keying, (DQPSK), modulation scheme with Square Root Raised Cosine, (SRRC), pulse shaping. This linear modulation scheme encodes baseband information in both the amplitude and phase of the R.F. carrier and is employed to increase spectral efficiency. If significant intermodulation and distortion products are to be avoided, class A linear amplifiers or backed-off class AB amplifiers must be employed. However, high power linear class A amplifiers are generally inefficient and undesirable in systems where cost and heat dissipation are prohibitive factors, e.g. a cellular telephone basestation. To avoid the compromise of constraints between the regulatory spectral emission mask and amplifier efficiency, attempts have been made to harness the efficiency of non-linear saturated class AB amplifiers by various linearization techniques.

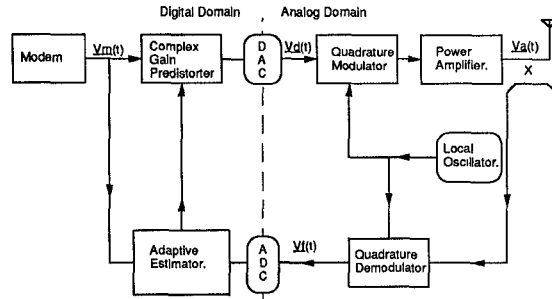
Experimental analog feedback techniques have been reported [1,2] but are generally limited to very narrow operating bandwidths, are extremely sensitive to amplifier variations, and prone to instability. Consequently these designs are not appropriate for mass production. Recently, simulation work has been presented [3,4] postulating the advantage of employing adaptive digital feedback at baseband. Such simulation work has promised excellent reduction in out-of-band spectral emissions, typically in excess of 25dB. These techniques are relatively insensitive to amplifier variations and provide an attractive design suitable for mass production. This paper presents the first experimental results, (to our knowledge) in which an adaptive complex gain predistorter achieves a reduction in out-of-band spectral emissions in excess of 20 dB for a class AB amplifier operating close to saturation.

II. Overview:- Complex Gain Predistortion.

Figure 1 illustrates the software/hardware configuration for the adaptive linearization circuit. In addition to a normal power amplifier design, an RF coupler, quadrature demodulator, and analog to digital convertor have been included to form a feedback loop.

The signal designations refer to the complex baseband signals or the complex envelope of the bandpass signals, this notation being compatible with the original theoretical work [3].

Figure 1. Adaptive Linearization Circuit.



The complex gain predistorter modifies the baseband complex modulation envelope, $\underline{Vd}(t)$, to correct for the nonlinearities introduced by the power amplifier. The adaptive estimator compares the desired complex modulation envelope, $\underline{Vm}(t)$, with the measured complex modulation envelope, $\underline{Vf}(t)$, from the PA, and estimates the complex gain predistortion coefficients. It should be noted that $\underline{Vf}(t)$ is a scaled, rotated and delayed version of $\underline{Va}(t)$. The characteristics of the complex gain predistorter are chosen such that its nonlinearity is complementary to that of the power amplifier. The original modulation trajectory is mapped to a new trajectory in the complex modulation plane by the characteristics of the predistorter. This new trajectory is chosen such that upon amplification by the non-linear PA, it is mapped back to the original and desired modulation trajectory. As a result the distortion and intermodulation products are eliminated, since the PA output is now constrained to the spectral characteristics of the linear modulation scheme.

The proposed complex gain predistortion technique [3] assumes that the amplifier may be characterized by memoryless Amplitude-to-Amplitude and Amplitude-to-Phase nonlinearities. This is represented by,

$$\underline{Va}(t) = \underline{Vd}(t) \cdot G(|\underline{Vd}(t)|^2) \quad -1$$

where $\underline{Vd}(t)$ and $\underline{Va}(t)$ are complex baseband representations of the instantaneous input and output complex modulation envelopes of the PA. The complex gain $G(|\underline{Vd}(t)|^2)$ defines the nonlinear amplifier gain to be a function of instantaneous input amplitude. This eases the computation of the adaptive estimator which seeks the predistortion coefficients. The complex gain predistorter is described by a similar complex gain equation,

$$\underline{Vd}(t) = \underline{Vm}(t) \cdot F(|\underline{Vm}(t)|^2) \quad -2$$

where $\underline{V}_m(t)$ and $\underline{V}_d(t)$ are complex baseband representations of the instantaneous input and output complex modulation envelopes of the predistorter. The characteristic function of the predistorter, $F(|\underline{V}_m(t)|^2)$, is estimated by the adaptive estimator which minimizes a simple loop error vector. This loop error vector is defined by eqn. 3 as the difference between the actual complex modulation envelope of the PA and the desired modulation envelope.

$$\underline{V}(\text{error}) = \underline{V}_a(t) - \underline{V}_m(t) \quad -3$$

III. The Adaptive Estimator.

A direct link may be established between the loop error vector and the characteristic function of the predistorter by eliminating $\underline{V}_d(t)$ from equations 1 and 2 and then substituting for $\underline{V}_a(t)$ in equation 3. Thus the error vector is rewritten, such that,

$$\underline{V}(\text{error}) = \underline{V}_m(t) \cdot F(|\underline{V}_m(t)|^2) \cdot G(|\underline{V}_m(t)|^2) \cdot F(|\underline{V}_m(t)|^2) - \underline{V}_m(t) \quad -4$$

The task of the adaptive estimator is to calculate the characteristic function, $F(|\underline{V}_m(t)|^2)$, of the predistorter such that for all values of $\underline{V}_m(t)$, the loop error vector, $\underline{V}(\text{error})$, is zero. A convenient method of representing $F(|\underline{V}_m(t)|^2)$ is to introduce a one-dimensional quantized look-up-table, which is indexed by the modulus of the baseband complex modulation envelope. As a direct consequence of the quantization it is assumed that the amplifier's AM-AM and AM-PM nonlinear characteristics are constant over the width of the table entry and invariant with phase. The corresponding table entry is a complex number representing the complex gain required to predistort the complex modulation envelope, $\underline{V}_m(t)$, for that specific instantaneous amplitude. The effects of table size and quantization step have been examined [3], and it has been demonstrated that look-up-tables of 32 and 64 entries provide sufficient spectral control of a non-linear amplifier when used in conjunction with a 16 level QAM modulation scheme. However, since the power amplifier's non-linear characteristics are a function of temperature, frequency, operating point and aging, the contents of the look-up-table must be continually updated to ensure accurate predistortion. The secant method has been proposed [3] as the basis for the adaptive estimator. However, initial experience with this algorithm has highlighted its sensitivity to incorrect initial conditions which can prevent convergence. Consequently, a less complex linear convergence technique known as **Rotate and Scale**, (RASCAL), has been developed for the adaptive estimator.

The adaptive estimator updates the predistortion look-up-table by continually comparing the original complex modulation envelope, $\underline{V}_m(t)$, with the sampled feedback complex modulation trajectory, $\underline{V}_f(t)$. As mentioned previously the feedback signal is a delayed version of the amplifier's output, $\underline{V}_a(t)$, and this delay must be eliminated before comparisons can be made. To estimate and remove the delay several techniques are available [4,5] and these are discussed in the next section. To effect the comparisons and update the look-up-table, the loop error vector, $\underline{V}(\text{error})$, is broken into magnitude and phase error equations,

$$\underline{V}(\text{error}) = \underline{V}_a(t) - \underline{V}_m(t) = |\underline{V}(\text{error})| e^{j\phi(\text{error})}$$

Converting to polar co-ordinates, two orthogonal error functions are defined,

$$\begin{aligned} e_{\text{scale}}(|\underline{V}_m(t)|^2) &= |\underline{V}_a(t)| - |\underline{V}_m(t)| & -5a \\ e_{\text{rotate}}(|\underline{V}_m(t)|^2) &= \arg(\underline{V}_a(t)) - \arg(\underline{V}_m(t)) & -5b \end{aligned}$$

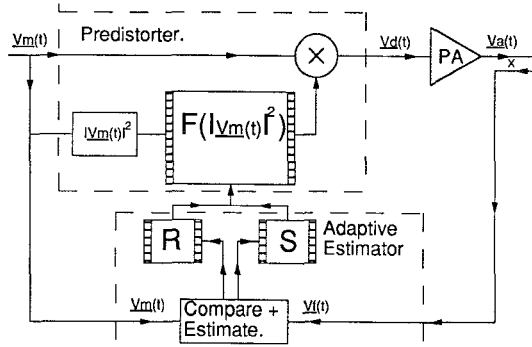
For all inputs to the amplifier of identical instantaneous signal amplitude, the scaling and rotational distortion, (AM-AM and AM-PM), is identical.

Consequently, the adaptive estimator must seek the correct complementary rotation and scaling to compensate for the amplifier. This is achieved by employing an iterative linear convergence to minimize the error functions defined by equations 5a and 5b. The adaptive estimator is defined by equations 6a,b, and the combined predistorter / adaptive estimator structure is illustrated in figure 2.

$$\begin{aligned} S_{\text{new}} &= S_{\text{old}} - \alpha \cdot e_{\text{scale}}(|\underline{V}_m(t)|^2) & -6a \\ R_{\text{new}} &= R_{\text{old}} - \alpha \cdot e_{\text{rotate}}(|\underline{V}_m(t)|^2) & -6b \end{aligned}$$

where α is the update gain which controls the rate of convergence and is usually restricted to be less than unity, and the subscript "old" refers to a specific table entry. This iteration occurs every instant that the complex modulation envelope traverses a given table entry. Each time a new rotate, R_{new} , and scale, S_{new} , factor is estimated they are recombined to form the complex gain of the predistorter, $F(|\underline{V}_m(t)|^2)$, and stored in the look-up-table. This technique is directly analogous to proportional and integral feedback familiar to control engineers.

Figure 2. Adaptive Estimator / Predistorter Structure.



IV. Loop Delay Estimation.

As mentioned in the previous section, the sampled signal, $\underline{V}_f(t)$, is a delayed version of the amplifier's output, $\underline{V}_a(t)$. Compensation for this delay must be made if the adaptive estimator is to compare $\underline{V}_m(t)$ and $\underline{V}_a(t)$ correctly. A delay compensation algorithm has been proposed [4]; however experimental experience has shown that distortion can significantly impair the accuracy of the delay estimate. A simple alternative for accurate delay estimation can be achieved by exploiting the properties of the modulation scheme [5]. For many digital modulation schemes a periodic component is generated at the symbol frequency if a strong non-linearity is encountered. Furthermore the phase of this periodic component is directly proportional to the incurred delay. The delay may be calculated by considering the following. Equation 7 defines an arbitrary linear digital modulated waveform, where a_i is a given symbol, $p(t - it - t_d)$ is the pulse shaping function, τ is the symbol rate, and t_d the delay to be estimated.

$$r(t) = \sum_i a_i \cdot p(t - it - t_d) \quad -7$$

Applying a strong non-linearity, for example a squaring function, leads to,

$$\begin{aligned} |r(t)|^2 &= r(t) \cdot r^*(t) = \sum_{ij} a_i \cdot a_j \cdot p(t - it - t_d) \cdot p^*(t - jt - t_d) \\ &= \sum_i |a_i|^2 \cdot p(t - it - t_d)^2 + \sum_{i \neq j} a_i \cdot a_j \cdot p(t - it - t_d) \cdot p^*(t - jt - t_d) \end{aligned}$$

Ignoring the second term since this does not contribute to the generation of the periodic component, simplifies the above equation to,

$$|I_r(t)|^2 = \sum_i |a_i|^2 |p(t - i\tau - t_d)|^2 \quad -8$$

Equation 8 may be redefined by extracting the delay via the delta function and removing $|a_i|^2$ from the summation since this is unity for all symbols in the $\pi/4$ DQPSK modulation scheme. Thus,

$$|I_r(t)|^2 = \sum_i |p(t - i\tau)|^2 * \delta(t - t_d) \quad -9$$

Taking the discrete frequency Fourier transform of equation 9 at $\omega_0 = 2\pi/\tau$ yields,

$$\mathcal{F}[|I_r(t)|^2] = \mathcal{F}[\sum_i |p(t - i\tau)|^2] e^{j\omega_0 t d} \quad -10$$

Since $\sum_i |p(t - i\tau)|^2$ is a periodic and even function of time, the Fourier transform $\mathcal{F}[\sum_i |p(t - i\tau)|^2]$ is a real quantity. Hence from equation 10,

$$\arg\{\mathcal{F}[|I_r(t)|^2]\} = -\omega_0 t d$$

and rearranging gives,

$$t_d = -\tau/2\pi \arg\{\mathcal{F}[|I_r(t)|^2]\} \quad -11$$

The application of the discrete frequency Fourier transform, DFFT, is straightforward in DSP. However to ensure correct delay estimation, the DFFT must be synchronized with the original modulation $V_m(t)$ to maintain an absolute zero time reference. Experimentally this technique has achieved an accuracy of $\pm 1/100$ of a symbol period, exceeding the recommended [4] accuracy of $\pm 1/64$ of a symbol period. To achieve this accuracy the DFFT was performed upon 2000 samples which corresponds to 200 symbols, which are sampled 10X. Experimental and simulation work has demonstrated that the accuracy of the technique is insensitive to power amplifier distortion. Since the samples are taken at discrete time intervals, typically $\tau/10$, it is unlikely that the loop delay will be a convenient multiple of the sampling rate. To achieve correct comparisons between $V_m(t)$ and $V_a(t)$, the sampling instants may be delayed in hardware by the calculated loop delay t_d . An elegant alternative is to employ a software interpolation scheme to reconstruct $V_a(t)$ with the appropriate loop delay compensation.

V. Experimental Results and Discussion.

Experimental System:- An experimental system was constructed as in figure 1. The DSP processor was a Texas Instruments TMS320C30 platform with dual DAC/ADC ports. The quadrature modulator was an inhouse analog design, whilst the quadrature demodulator and RF coupler were standard commercial units. The power amplifier was a commercial 6 watt, class AB package specifically designed for the cellular frequency band. The modulation scheme was $\pi/4$ DQPSK, (with raised cosine pulse shaping and a rolloff factor =0.35), running at a bit rate of 2000 bits/s and 10x sampled. The local oscillator frequency was set at 857MHz.

Experimental Procedure:-

The power amplifier was driven to the saturation point and then backed off by 1 dB. The RF spectrum was recorded for the operating condition. The experiment was then repeated with the adaptive complex gain predistorter running, which was allowed to converge and the RF spectrum recorded. For both experiments the inband RF output power was maintained at a constant level.

Experimental Results:-

Early experimental results indicated that the complex gain predistorter could achieve a modest 10 dB reduction in spectral distortion. This performance was disappointing when compared to the simulation results which had indicated that an excess of 25 dB could be achieved. Examination of the baseband demodulated $\pi/4$ DQPSK constellation revealed that an apparent phase-dependent distortion mechanism was present. Successful operation of the complex gain predistorter is dependent upon a memoryless AM-AM and AM-PM nonlinear distortion mechanism; unfortunately the observed distortion violates this assumption, as discussed below. The apparent phase dependent distortion mechanism has been isolated and can be attributed to local oscillator carrier feedthrough. Ordinarily, LO carrier feedthrough is regarded as a simple nuisance causing the generation of a DC term upon demodulation. However, close examination of the R.F. carrier envelope that is formed by the combination of the $\pi/4$ DQPSK modulation scheme and the LO carrier feedthrough reveals the distortion mechanism. Equation 12a represents the $\pi/4$ DQPSK R.F. carrier, equation 12b represents the LO feedthrough which has some constant but arbitrary amplitude and phase.

$$RF(t) = I(t) \cos(\omega t) - Q(t) \sin(\omega t) \quad -12a$$

$$LO(t) = A \cos(\omega t + \phi) \quad -12b$$

The combined R.F. carrier is formed by linear superposition,

$$S(t) = RF(t) + LO(t) = I(t) \cos(\omega t) - Q(t) \sin(\omega t) + A \cos(\omega t + \phi)$$

Trigonometric manipulation gives

$$S(t) = (I(t) + A \cos(\phi))^2 + (Q(t) + A \sin(\phi))^2^{1/2} \cos(\omega t + \Phi) \quad -13$$

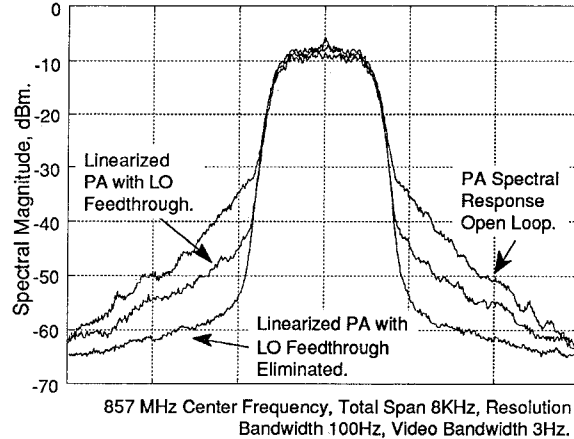
$$\Phi = \tan^{-1} (Q(t) + A \sin(\phi)) / (I(t) + A \cos(\phi))$$

Close examination of equation 13 reveals that for a locus of constant modulus in the IQ complex modulation plane, the corresponding amplitude of the R.F. carrier, $S(t)$, is not constant. This is contrary to the expected constant envelope; the fluctuations are a direct result of the $A \cos(\phi)$ and $A \sin(\phi)$ terms in equation 13. This situation may be envisaged in the complex modulation plane as a translated $\pi/4$ DQPSK constellation. However, the instantaneous magnitude of the R.F. carrier is still referred to the origin, and as a consequence, trajectories of identical magnitude, when referred to the constellation center, no longer suffer identical AM-AM and AM-PM distortion. This immediately undermines the operation of the complex gain predistorter which assumes all modulation trajectories of constant magnitude, when referred to the constellation center, suffer identical AM-AM and AM-PM distortion. Therefore LO carrier feedthrough immediately defines a fundamental limit to the reduction in spectral distortion that a complex gain predistorter may achieve. This limit is dependent upon two factors: the extent of LO feedthrough, and the AM-AM and AM-PM distortion characteristic of a given power amplifier.

LO carrier feedthrough may be reduced by employing an attenuator and phase shifter in parallel with the quadrature modulator. The phase shifter and attenuator are adjusted so that deliberate destructive interference occurs between the LO carrier feedthrough and the bypass carrier. The adjustment of the attenuator and phase shifter is currently done by hand and is achieved by observing that the distortion becomes uniformly distributed in the demodulated baseband constellation. Using this method the LO carrier feedthrough is reduced from -20 dBc to an estimated -40 dBc.

Although this is a crude experiment, the comparison between the initial spectral performance and the reduced LO carrier feedthrough spectral performance, (as shown in figure 3), achieved by the complex gain predistorter is significant. A further increase of 10 dB has been achieved, yielding a total reduction in spectral distortion in excess of 20 dB.

Figure 3. Complex Gain Predistorter Performance With and Without Local Oscillator Feedthrough.

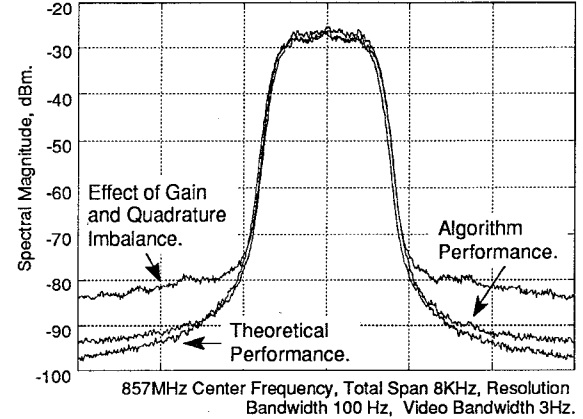


VI. Discussion of Results

The experimental results clearly demonstrate that the power amplifier may be linearized without sacrificing efficiency. The experiment also confirms the original assumption, that the power amplifier may be described by a memoryless AM-AM and AM-PM non-linearity, is correct. Unfortunately, the phase shifter and attenuator are not desirable in a commercial system. This places great emphasis upon the modulator design which should achieve a LO carrier feedthrough of less than -40 dBc. In practice this is difficult to achieve in high volume commercial designs.

Although significant spectral reduction is achieved in the adjacent channel, careful examination of figure 3 reveals that the out-of-band spectral floor is flat and approximately -50 dB from the inband spectra. Depending upon the application, this may exceed the alternate channel regulatory spectral emission mask. The magnitude of the out-of-band spectral floor is governed by the imperfections of the quadrature modulator and demodulator. Accurate operation of the complex gain predistorter is dependent upon perfect quadrature, (ie 90°), modulation and demodulation, and zero gain imbalance between the I and Q channels. Practical analog components are typically specified at $\pm 30^\circ$ phase imbalance and ± 0.2 dB gain imbalance. It is these imperfections that limit the out-of-band spectral reduction achieved by the complex gain predistorter. To demonstrate this reduction in potential performance, figure 4 compares theoretical spectrum with the algorithm performance with and without the inclusion of the RF imperfections. The lowest spectral trace corresponds to the theoretical performance, the middle trace corresponds to the RASCAL algorithm operating when $V_f(t)$ has been derived from baseband feedback only. The slight degradation is due to quantization error and minimal channel imbalance through the DAC/ADC. The highest trace corresponds to the RASCAL algorithm operating when $V_f(t)$ has been derived from an RF feedback loop without a power amplifier. The degradation in spectral performance, (typically >10 dB), is significant; clearly the quadrature and gain imbalances of analog components is critical to successful operation.

Figure 4. Effect of Quadrature and Gain Imbalance upon Complex Gain Predistorter Performance.



VII. Conclusions.

The experimental results clearly demonstrate that a class AB power amplifier may be linearized without sacrificing efficiency. Although significant reduction of spectra, (>20 dB), in the adjacent channel is achieved, careful examination of figure 3 reveals that spectral in the alternate channel does not decay. Depending upon the regulatory spectral emission mask for a given application, this may or may not present a difficulty. The complex gain predistorter exhibits two distinct advantages:

- I. a design engineer is not forced to back off a power amplifier to its linear but highly inefficient operating point.
- II. adaptive correction allows the effects of frequency changes, drift in bias, operating point, aging and thermal stress to be readily compensated.

This technique provides the basis for a reliable design suitable for inclusion in a mass manufactured system, such as a cellular basestation.

VIII. References.

1. "Linear Transceiver Architectures." A.Bateman, D.M.Haines and R.J.Wilkinson. IEEE Proceedings Vehicular Technology ConferencePhiladelphia IEEE 1988 Catalog No. 2622-9/88/0000-0478 pp478-484.
2. "Feedforward Linearization of 950MHz Amplifiers." R.D.Stewart and F.F.Tusubira. IEE Proceedings Vol 135 Pt H No.5 October 1988
3. "Amplifier Linearization Using a Digital Predistorter with Fast Adaptation and Low Memory Requirements" James K. Cavers IEEE Transactions on Vehicular Technology. Vol39 No4 Nov. 1990.
4. "Linear Amplification Technique for Digital Mobile Communications." Yoshinori Nagata. IEEE Proceedings Vehicular Technology Conference. San Francisco 1989. pp159-164.
5. "Digital Communication." Edward A. Lee and David G. Messerschmitt Kluwer Academic Publishers 1990. Chapter 15 pp 566-569.